Book of Tutorials and Abstracts

European Microbeam Analysis Society

EMAS 2023

17th

EUROPEAN WORKSHOP

on

MODERN DEVELOPMENTS AND APPLICATIONS IN MICROBEAM ANALYSIS

7 to 11 May 2023
at the
Jagiellonian University, Auditorium Maximum
Krakow, Poland

Under the auspices of the Rector of the
Jagiellonian University, Krakow, Poland
Organised in collaboration with the
Institute of Metallurgy and Materials Science of
the Polish Academy of Sciences, Krakow, Poland

EMAS
European Microbeam Analysis Society eV
www.microbeamanalysis.eu/

This volume is published by:
European Microbeam Analysis Society eV (EMAS)
EMAS Secretariat
c/o Eidgenössische Technische Hochschule, Institut für Geochemie und Petrologie
Clausiusstrasse 25
8092 Zürich
Switzerland

ISBN 978 90 8227 6961
NUR code: 972 – Materials Science

DEVELOPMENTS AND APPLICATION IN TRANSMISSION KIKUCHI DIFFRACTION

Tomasz Tokarski

AGH - University of Science and Technology, Academic Centre for Materials and Nanotechnology
Al. Mickiewicza 30, 30059 Krakow, Poland
e-mail: tokarski@agh.edu.pl

Tomasz Tokarski's background comes from the field of materials science of non-ferrous metals and alloys. After completing his PhD thesis in 2007, he started work at the AGH University of Science and Technology in the Faculty of Non-Ferrous Metals, and since 2016 in Academic Centre for Materials and Nanotechnology. Apart from his scientific duties, he is also working with companies related to the industry, particularly within the field of high pressure die casting and the development of aluminium alloys for forging applications. His interest in the field of electron microscopy started from his PhD work, where he investigated dislocation structure transformation in FCC metals. The following years brought increased interest in SEM and SEM-EBSD/TKD methodology. Over the last 15 years, he was a co-author of more than 100 scientific papers. Currently, he is sharing his time between industrial activities and scientific work in the field of electron microscopy. His current scientific work is focussed on the development of CALM (crystallographic analysis of the lattice metric) software for the solution of unknown phases using EBSD/TKD diffraction.

1. ABSTRACT

Transmission Kikuchi diffraction (TKD) is a fairly new technique, significantly improving the spatial resolution of the electron-back scattering diffraction (EBSD) methodology. It combines thin foil samples with the widely available EBSD camera systems allowing for efficient analysis of light materials at the nanoscale.

Over approximately ten years, TKD technique has gained more traction, primarily due to the equipment availability and well-developed sample preparation routines. The paper presents a short description of TKD technique, particular physical limitations and geometrical constraints of acquisition setup as well as typical conditions used during analysis. Several papers were published about the technique itself; however, there is almost no information on how to properly set up both the microscope and the camera system to achieve the best results. The goal of the paper is to demonstrate how easily the TKD technique can be employed in a standard laboratory routine resulting in spatial resolution improvement without sacrificing the efficiency of EBSD system.

2. INTRODUCTION

The electron backscatter diffraction EBSD technique is a well-established methodology for the analysis of crystalline materials. Utilisation of a focused electron beam enables local analysis of material crystallinity, which is impossible to achieve by commonly used X-ray based techniques. Over the years, continuous improvement of the EBSD camera hardware and computer processing power resulted in a significant reduction of time needed to acquire maps – from hours to just a few minutes. Despite obvious advantages, the spatial resolution of standard EBSD methodology is limited by the physical effects of the electron-matter interaction volume. The limitation became a major factor for the characterisation of materials in sub-micro and nano-scale.

Modern scanning electron microscopes equipped with field emission gun (FEG-SEM) are capable of focussing beams down to 1 nm diameter, which is well below limits imposed by EBSD methodology. The electron-material interaction volume is, therefore, a major obstacle to improve the EBSD spatial resolution.

The importance and discussion of achievable EBSD spatial resolution is a topic of many papers (see for example [1, 2]). Major factors affecting spatial resolution are average material atomic number and primary beam energy. Favourably, the source of the useful diffraction signal is located just below the specimen surface, at depth ranging from several nanometre to several tenths of nanometres [3]. Electrons emerging from the deeper layers of the material contribute mainly to the diffusive background of the Kikuchi pattern [4]. Nonetheless, low-Z materials have an inferior spatial resolution which can be as low as 100 nm rendering mapping of nanometre-size microstructure features hard or even impossible. An obvious way for spatial

resolution improvement is the utilisation of lower beam energy. It is possible to run an experiment with accelerating voltage as allow as 5 kV, however slower acquisition time and high sensitivity for carbon build-up during analysis significantly reduces the usability of such solution [2].

A novel approach for spatial resolution improvement, presented for the first time in 2012, was to use a TEM-like thin specimen instead of a bulk one [5, 6]. Significant improvement in resolution was achieved by the physical reduction of sample thickness and electron-matter interaction volume. New acronyms were coined for the new technique from which TKD (transmission Kikuchi diffraction) or t-EBSD (transmission-EBSD) are most common in the literature [7].

An example of resolution improvement in light material mapping is presented in Fig. 1. All maps were acquired with the same step size of 50 nm and no map cleaning is applied. While accelerating voltage decrease causes visible improvement for EBSD analysis, spatial resolution is still inferior in comparison to the TKD case. It is particularly well visible in the image quality (IQ) maps where grain boundaries are very sharp, often with a thickness of one pixel.

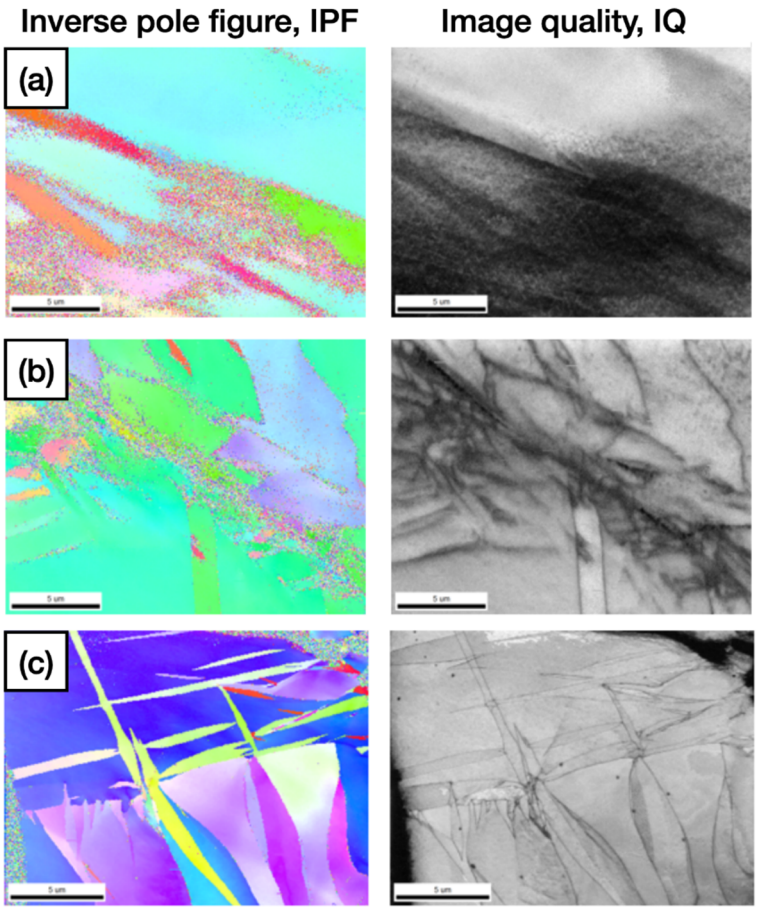

Figure 1. Comparison of the IPF and IQ maps acquired for the deformed magnesium sample: a) EBSD 20 kV, b) EBSD 10 kV and c) TKD 20 kV.

Besides an order of magnitude spatial resolution improvement, TKD methodology is strongly supported by the application of EBSD acquisition equipment as well as widely available data processing software packages. In other words, any laboratory equipped with FEG-SEM and EBSD camera system is capable of using TKD technique. The additional cost needed to run transmission mode measurements is minimal, as it requires only a dedicated specimen holder and the application of thin foil preparation techniques to the laboratory routine. All the above makes TKD a very powerful technique, extending broadly available EBSD methodology into the nanometre-scale regime.

There are many books, papers and courses dealing with the EBSD technique from which information can be directly applied to TKD methodology. An extensive review of applications for TKD technique is also provided in the literature [8]. Nonetheless, there are specific details of TKD methodology, essential for correct acquisition system setup, which will be addressed further below.

3. *ACQUISITION GEOMETRY*

Thin foil samples used in TKD experiments require a different sample-camera geometry. During EBSD analysis, the inclined sample surface is facing towards the camera registering backscattered electrons (Fig. 2a), while TKD requires the sample to be positioned close to the SEM pole-piece, registering only transmitted electrons. Both configurations use standard camera systems with vertical or near-vertical alignment of the phosphor screen. An alternative solution employs a dedicated camera head with horizontal position of the phosphor screen. Depending on the geometry of the acquisition system, particularly the location of the phosphor screen with respect to the primary beam, two distinctive abbreviations are commonly used: off-axis TKD (Fig. 2b), and on-axis TKD (Fig. 2c). To the best of my knowledge, most working systems are standard EBSD cameras applied to the TKD methodology (off-axis setup), while the number of the on-axis system is limited, being supported by a single manufacturer of camera system only.

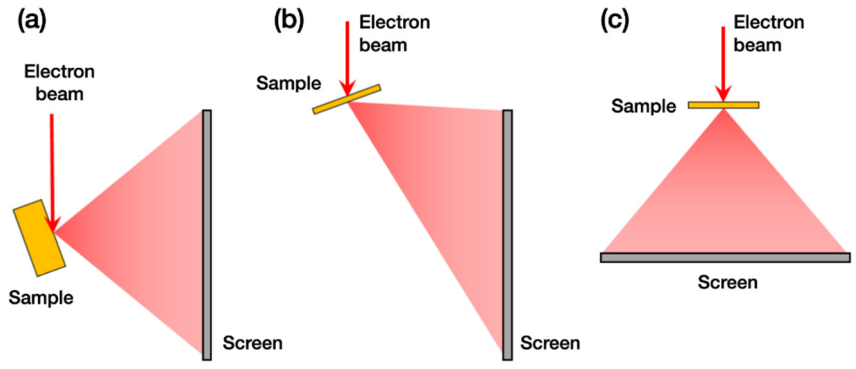

Figure 2. Comparison of the geometry of EBSD and TKD setups. Acquisition geometry of a) EBSD, b) off-axis TKD, and c) on-axis TKD. D) Definition of the projection centre PC as a point source of diffraction.

An important parameter of EBSD setup is the projection centre (PC = {PC_x, PC_y, PC_z}), which defines the position of the camera screen with respect to the source of diffracted electrons. Following PC definition typical EBSD analysis, presented in Fig. 3c, is performed for the PC_z in the range of 0.5 to 0.8, PC_y is in the range of 0.3 to 0.6, and PC_x is located around 0.5. It is important to mention, that the correct PC is needed for the indexation routines, and it should be optimised experimentally for each given sample position.

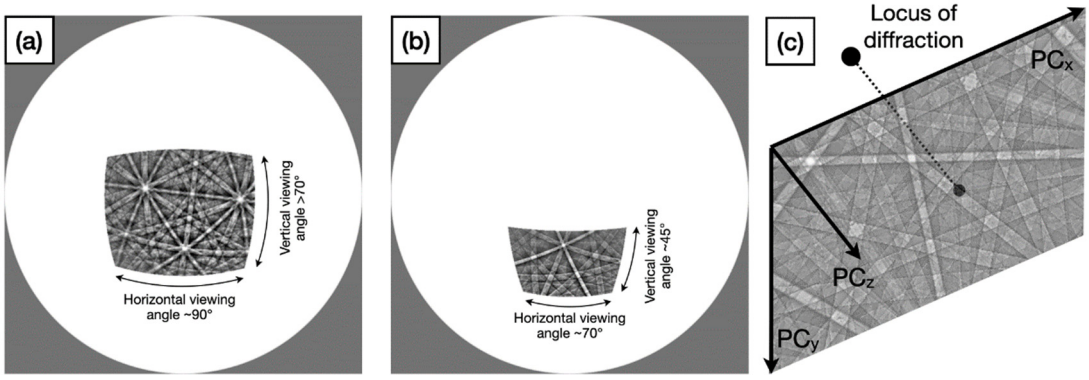

Figure 3. Stereographic projection of a) EBSD, and b) off-axis TKD setup showing visual information of the camera viewing angle. D) Definition of (PC) used in the paper.

One of the characteristics of standard EBSD is that the position of PC is providing a wide-angle view of the diffracted signal. For typical acquisition conditions, the angle of view (in the vertical direction) is greater than 70° allowing for registration of many reflectors (Kikuchi bands) simultaneously. A large field of view is one of the biggest advantages of EBSD systems providing high reliability and/or precision of the measurement.

The off-axis TKD system, however, due to the diffraction locus set above an upper edge of the camera, is characterised by significantly decreased angle of view (Fig. 3b). Both EBSD and TKD configurations are qualitatively compared in Fig. 3.

The lower PC_y used, the smaller the part of the diffracted signal is registered by the camera. In a typical off-axis TKD acquisition setup, the PC_y-value should be negative, preventing the shadowing effect of the sample. In practice, PC_y-values in the range of -0.1 to -0.3 are used, which reduces the vertical viewing angle to the value of approximately 45°. In certain situations, lower reflector numbers available for the camera system can give false or no solutions, which have to be addressed by optimisation of indexation routine parameters.

Another feature inherent to the registered patterns is a gnomonic distortion of the Kikuchi bands [9]. Most of the systems employ Hough/Radon transformation for band detection, where bands are commonly approximated by a pair of straight lines. Having a PC_y close to the centre of the

pattern makes such an assumption justified. It is not the case in off-axis TKD where band distortion is much more prominent. An example is presented in Fig. 4 where the three-fold symmetry axis of the FCC pattern is positioned nearby the centre of the screen. While in the EBSD setup, the symmetry axis is easily recognisable, off-axis TKD case shows high distortions, where bands belonging to the same family are different in thickness and the symmetry in the image is lost. Both the image distortions and exceptionally broad Kikuchi bands can have an adverse impact on the peak recognition algorithm via Hough/Radon transformation.

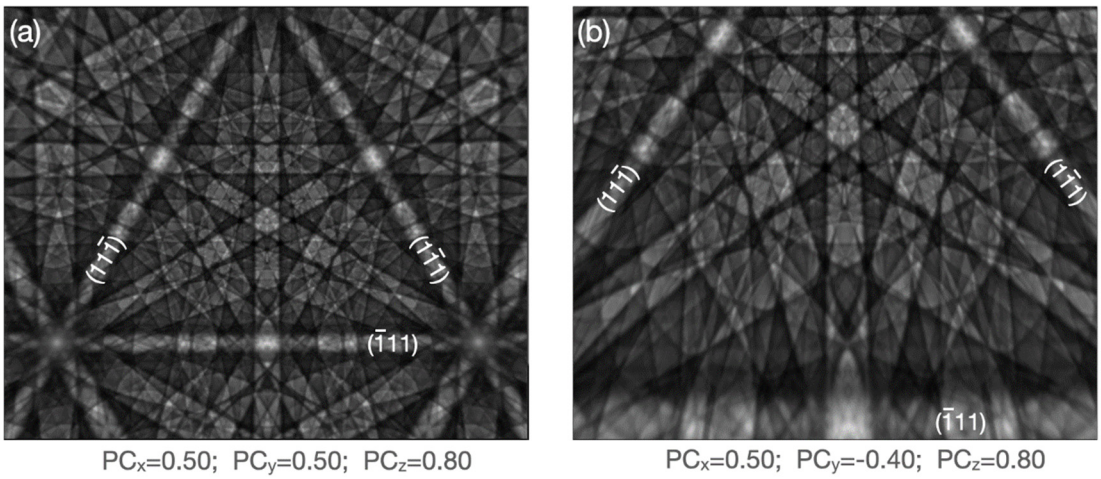

Figure 4. Gnomonic distortions of the pattern due to various PC position: a) EBSD and b) off-axis TKD. Origin of PC is defined in the left upper corner of the image with "y" value pointing down, i.e., a negative PC_y-value positions the diffraction locus above the image.

Commercially available indexing software packages are delivered in the form of a "black-box" solution, often without information about algorithm workflow. Most of the image processing pipeline is hidden from the users, thus it is impossible to judge the impact of gnomonic distortions on the final orientation solution; however, even in the presence of clear/sharp pattern features, the software can fail to correctly solve phase or orientation.

4. SIGNAL INTENSITY AND HOLDER DESIGN

Another feature that is strongly affected by the PC position is the signal intensity registered in the camera. In the EBSD system, sample tilt with respect to the primary beam angle is set at approximately 70°, giving a good compromise between signal intensity, pattern quality and spatial resolution.

The camera in TKD is operating in transmission mode where most of the electrons are only slightly deviating from the primary beam direction. A significantly limited electron-matter

volume improves the spatial resolution, but it also substantially reduces the number of electrons scattered at larger angles resulting in the low signal intensity registered in the phosphor screen. The number of scattering events in a thin sample is dependent on the sample thickness, the average atomic number, and the primary beam energy. Lighter material, lower material thickness and higher accelerating voltage are reducing the signal level in the camera screen. At the same time, the mentioned direction of parameter change is having positive effect on spatial resolution.

To present variations of the signal intensity in the camera, it is convenient to represent the number of transmitted electrons as a function of scattering angle. Figure 5 is an example of Monte Carlo simulations for Mg thin foils with varying thickness and an accelerating voltage of 30 kV. The vertical axis values are normalised to the unit and presented on a logarithmic scale. Additionally, the camera viewing angle in the vertical direction is marked in pink colour. As expected, the highest intensity of the transmitted signal is following the primary electron beam direction with continuous drop with increasing scattering angle. In fact for the 50 nm thin magnesium foil, 99 % of electrons are confined within a cone with an opening angle of 1°. The available signal for the camera is, therefore, very low, having an intensity reduced by a factor of approximately 10^{-3} and $5 \cdot 10^{-5}$ for the lower and upper of the camera screen region respectively.

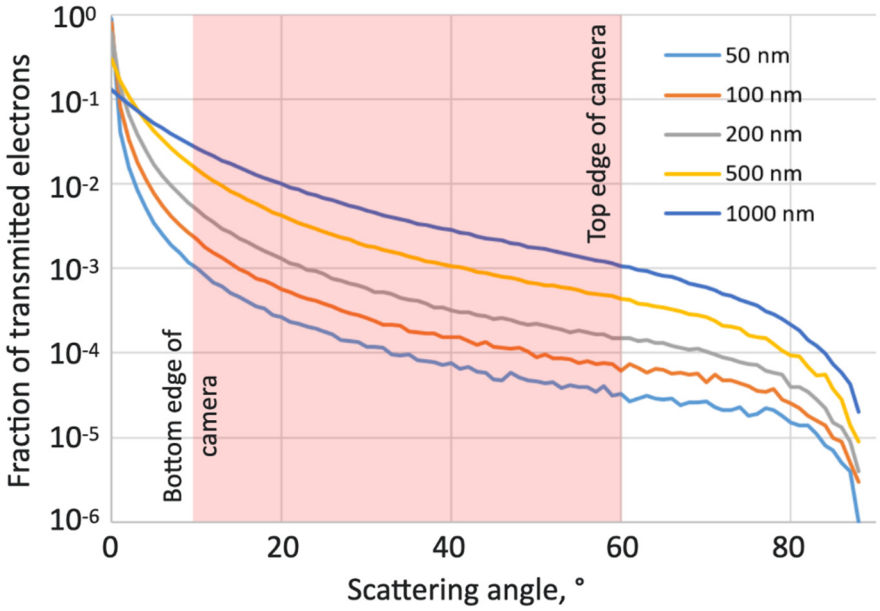

Figure 5. Fraction of transmitted electron as a function of scattering angle for various thickness of a magnesium foil and constant accelerating voltage of 30 kV.

One of the adverse consequences of the off-axis TKD methodology is thus very low signal intensity, which can significantly reduce camera acquisition by a factor of 10 in comparison to the EBSD case.

During EBSD analysis strong background signal reduces the dynamic range available for the diffracted signal, therefore, to obtain the best performance of the indexation routine, parameters of the acquisition system are set to achieve an almost fully saturated camera. Such an approach is no longer needed for TKD analysis. Small energy losses in the thin foil [10, 11] directly translate to a less intense and noisy background and acquiring useful/diffraction signal with the same dynamic range, which in EBSD case requires much lower camera intensities. Tests performed with an Hikari EDAX camera are showing that recognisable Kikuchi bands can be obtained utilising only 2 % of the total camera intensity range only [12]. A significant reduction of the camera integration time is thus possible without adverse effects on the pattern indexation reliability.

The major drawback of low-intensity measurements, however, is a substantially increased sensitivity to any electrons re-scattered from the specimen holder. Most of the transmitted electrons are scattered at low angles, thus any holder surface below the thin foil will act as an additional source of re-scattered electrons, which are contributing to the pattern background. The analysis of patterns registered with different background levels shows that re-scattered electrons can increase the noise level by a factor of five [12]. The individual value of the noise level is dependent on the specimen-holder geometry, material being analysed, accelerating voltage and foil thickness. The simplest solution is to apply a dedicated shield, effectively blocking all unwanted electrons. Although such a solution seems to be obvious, many publications show custom-made holder solutions with the surfaces exposed directly to the transmitted beam [11, 13, 14]. Other tapered holder solutions can alleviate the problem by minimising holder surfaces exposed to the transmitted beam [15]. The shield, however, can be added to any configuration, creating more flexibility in holder design. An example of a shielded holder used during TKD analysis is presented in Fig. 6. Shielded solution proved to be very effective and by utilising low camera saturation levels enables full camera acquisition speeds for heavy elements and up to half of the full camera speed for light elements [16].

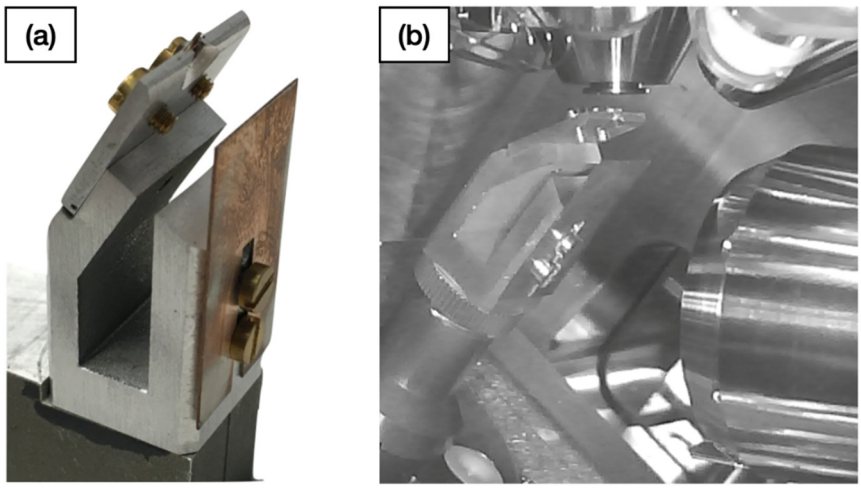

Figure 6. Custom made holder with dedicated shield: a) holder view with copper shield, and b) position of the holder in from of the camera.

5. *SPATIAL RESOLUTION OF MEASUREMENT*

Spatial resolution improvement of TKD measurements starts from the application of TEM-like specimen. Considering the electron-matter interaction volume, usual measurement parameters such as material type, and accelerating voltage have the opposite effect as in the EBSD technique. Higher accelerating voltage and lower material atomic number will result in better spatial resolution. Similar improvement is expected when decreasing sample thickness. Absolute limits of spatial resolution are difficult to measure as those depend on multiple factors originating from the measurement methodology and hardware/software used. Additionally, the asymmetric position of the camera with respect to the sample in EBSD and off-axis TKD, leads to the two different resolution parameters [2]. Measurement of the spatial resolution is usually performed across a specifically oriented grain boundary. At some point, excitation of both of the grains will result in pattern overlap, which can be detected by image cross-correlation or by changes in the pattern quality index. There are two types of spatial resolution parameters used, namely physical and effective resolution [2]. While the first one can be defined by the closest position to the grain/phase boundary with the excitation of one grain only (analysis via cross-correlation), the second includes software system capability for deconvolution of overlapping patterns (analysis via pattern quality metric).

Experimental measurements of the EBSD or TKD resolution is a complex problem where multiple parameters have to be considered simultaneously. Alternatively, Monte Carlo simulations can be used to effectively estimate the impact of the selected acquisition parameters on the beam spread in a thin sample. An example of calculated spatial resolution for the TKD system is presented in Fig. 7.

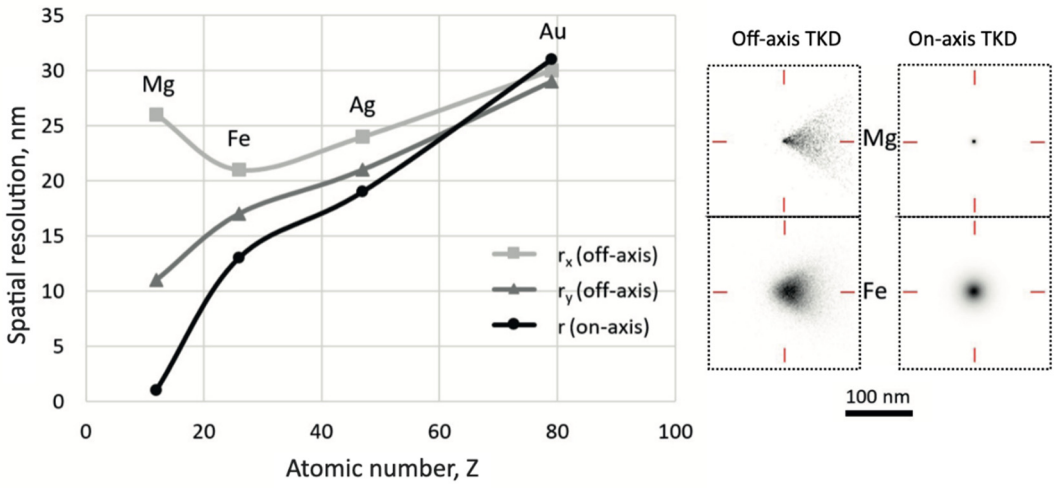

Figure 7. a) Results of Monte Carlo simulations of spatial resolution performed for materials with various atomic number, with an accelerating voltage of 30 kV and a sample thickness of 100 nm. b) Distributions of transmitted electrons registered in the detector at the exit surface of 50 nm thin foils.

For calculations, only the electron trajectories leaving the bottom surface of the foil towards the camera screen were used. An assumption was made that the inelastic scattering events contributing to diffracted signals originate close to the exit surface of the thin foil [11]. Examples of the electron spread at the surface of the foil are presented in Fig. 7. Due to the side position of the camera in the off-axis case, the spread of the electrons registered in the detector is not symmetric, showing characteristic "comet-tail" distribution. It is particularly pronounced for light materials giving rise to the difference between spatial resolution parameters. On-axis TKD requires only one parameter, as the camera position does not break the axis symmetry of transmitted electrons.

Simulations are simplifications of real systems and thus cannot be used as a reference for absolute spatial resolution limits. Nonetheless, it can provide an important insight into the relative value change for different materials and acquisition parameters. For the light materials, the 10nm spatial resolution limit can be expected, which is in agreement with a typical value cited in the literature [15]. What is important to mention for materials with low atomic numbers on-axis setup is superior to the off-axis setup. As expected, due to increased electron-matter interaction volume, spatial resolution is deteriorated for heavier materials.

6. EXAMPLES OF OFF-AXIS TD MEASUREMENTS

The results presented in this chapter are selected to emphasise specific problems of the TKD technique. All maps were registered using an Hikaru EDAX camera and EDAX TEAM software. Only raw data are used without any map cleaning procedure applied.

Fig. 8 shows TKD maps of a coarse-grained stainless-steel sample. It shows that extraordinarily large ones are mapped around a thin foil perforation. The sample was prepared using twin-jet electropolishing and has a characteristic wedge-type thickness profile and significant thickness variations in the vicinity of the perforation. It is possible to map areas with thicknesses even up to 1 μm for heavy metals. In thicker regions, however, there is a significant drop in pattern indexation success as well as a deterioration of the image quality (IQ) parameter. For the best spatial resolution, measurement is usually performed in the thinnest possible region, located on the perforation edge where the IQ map is showing sharp grain/phase boundaries. With proper application of the electropolishing technique areas in the range of tens of micrometres can be effectively mapped.

The next example presents TKD maps of the same stainless-steel sample after 10 % of deformation at the temperature of -30 °C (Fig. 9). The scan step was set to 10 nm what allowed to map thin lamellas of deformation martensite. The thinnest features resolved (marked by white arrows) are approximately 10 nm thick and are only visible on the IQ map. Although smaller features are present and detectable, they cannot be de-convoluted from an overlapped pattern by the software and mapped as separate orientations/phases. The example also shows two typical

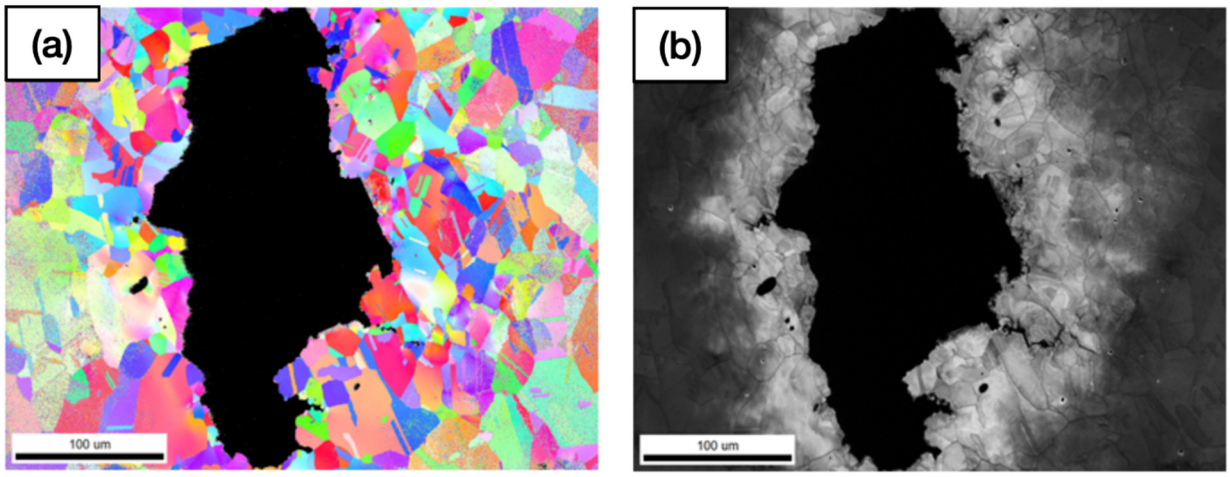

Figure 8. Coarse grained stainless-steel sample analysed around perforation. a) Inverse pole figure map, and b) Image quality map.

artefacts often occurring during TKD mapping, namely thin foil bending and carbon contamination built-up. Thin foil bending is a consequence of internal stress relaxation caused by the introduction of two free surfaces. It results in continuous local orientation changes and is particularly well visible on the IQ map in the form of slowly changing contrast in the left-upper part of the image (Fig. 9a). The second artefact, visible in the form of thin, dark vertical lines and darker spots in the IQ image, is caused by the carbon build-up process, and becomes more pronounced as scans is progressing towards bottom of image. In this particular case, contamination does not alter solutions of the orientation, nonetheless, it can constitute a limiting factor for the maps acquired with the very small step size.

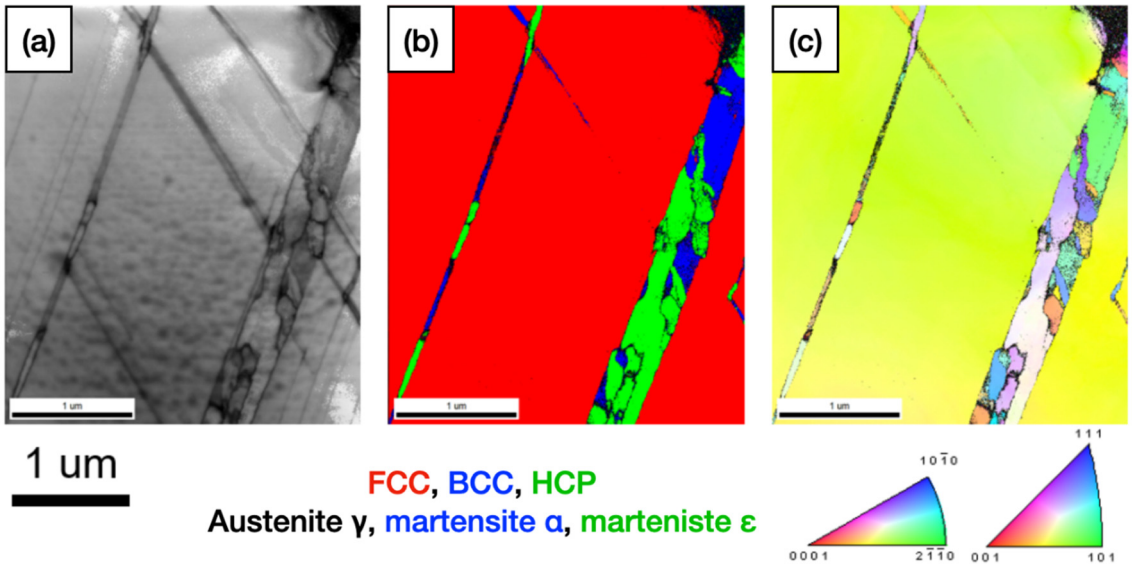

Figure 9. Deformed stainless-steel sample analysed around perforation. a) image quality map, b) phase distribution map, and c) inverse pole figure map.

The electropolishing technique is a very versatile and economical way of thin foil preparation of metallic materials. The best results can be obtained for one-phase materials, while multi-phase or non-homogeneous samples are usually unsuitable for the electrochemical process.

An alternative for thin lamella preparation is the focussed ion beam (FIB) technique. FIB allows site-specific preparation of complex microstructure materials. It is, however, expensive and requires skilled operator for sample preparation. An example of a FIB-prepared sample is presented in Fig. 10, showing a cross-section of the nitride, forming a nucleus for the spheroidal graphite growth [17]. Application of FIB was very difficult as the nitride is supported only by the thin brittle graphite part. Only a fragment is visible as half of the thin lamella was lost during sample transfer to the TKD holder. Finally, data were acquired to map nitride and graphite areas around it. Orientation solutions are only available for the nitride part of the sample and are presented in the form of an overlay over the IQ image. Nitride diffraction was of a very good quality and was easily indexed by the software. To the contrary, most of the graphite patterns, although having clear and distinct bands failed to index. It is a clear indication that a limited number of broad Kikuchi bands can be difficult to process by the software indexing routine.

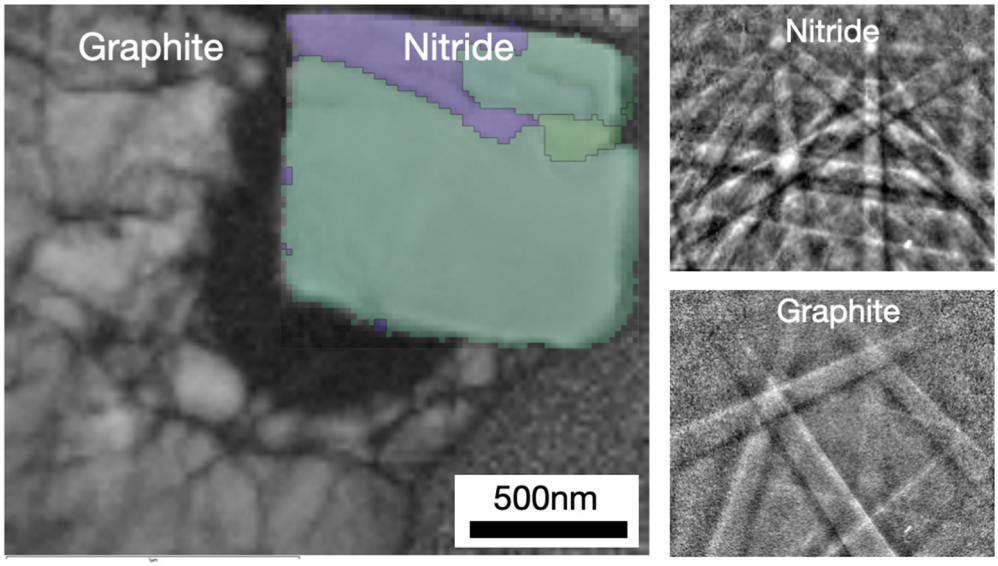

Figure 10. Cross-section of the nitride nucleus in the spheroidal graphite. Inverse pole figure overlay is only provided for the nitride part of the map.

7. FINAL REMARKS

Transmission Kikuchi diffraction is a blend of standard SEM equipment with thin samples well-known from transmission electron microscopy (TEM). If performed correctly it can be as productive as the conventional EBSD technique, enabling local measurement of crystallographic features of materials at the nanoscale. Whenever thin specimens can be prepared with one or

more dimensions smaller than several hundreds of nanometres, the TKD technique can be employed. The examples are not only limited to the thin foil analysis but also nano-particle or samples used in atom probe tomography (APT) experiments.

At this point, it is convenient to recapitulate potential problems that may be encountered during TKD measurement. In particular, the map acquisition speed is a critical factor – especially for maps with a step size of 10 nm to 20 nm. Too low speed is resulting in an issue of carbon contamination and mechanical instability of the microscope. Carbon contamination is dependent on sample's cleanness and chamber vacuum quality. Examples presented in the paper were acquired using SEM with a variable vacuum system and vacuum level of 10^{-3}Pa. To avoid contamination problems, map steps below 20 nm required acquisition speeds above 200 patterns per second (pps). Another issue inherently encountered with the TKD methodology is microscope mechanical stability. SEM stages are typically designed to support relatively big and heavy specimens, thus long-term drift, caused by backlash in the stage drive system, is often significant. High tilt conditions are most affected by mechanical instability, it is thus advised to use drift correction algorithms if available or to leave a microscope for several hours to stabilise. Another more robust option is to prepare the holder for work with zero tilt conditions keeping drive backlash at minimum. In such a case screening out of all electrons re-scattered by the horizontally aligned holder support can be easily accomplished by a simple shield plate. Acquisition speed can be improved by boosting the signal intensity and setting the camera to low-intensity conditions. Currents between 4 nA to 16 nA or higher are not unusual during an analysis of metallic samples. Camera intensity should be set to a low level of 10 % to 20 % of full camera saturation. In such conditions pattern preview mode using the raw camera image can show black or almost black image, thus it is mandatory to use dynamic, static background correction or intensity stretch routines to confirm pattern quality. It is convenient to acquire maps at the highest accessible accelerating voltage of the microscope, which is usually 30 kV. It brings the best spatial resolution, the possibility of imaging thicker specimen regions and, finally, narrower Kikuchi bands for line detection algorithms.

Final words are addressed towards the reliability of data obtained from TKD analysis. Besides typical problems and drawbacks of EBSD processing pipeline, the analysis of thin materials can produce additional artefacts resulting in incorrect results. Sample preparation for TKD analysis is a highly destructive technique. Creating large free surfaces from the bulk specimen by milling out significant portions of materials is changing the physical state of the system, which in turn can trigger dislocation structure changes or phase transformation phenomena. Additionally, high current beam conditions used during TKD analysis can act on the small sample causing radiation damage or a local rise in the temperature to the value, where diffusion effects or structural transformation can occur.

8. ACKNOWLEDGMENTS

I would like to express my gratitude to Gert Nolze, Aimo Winkelmann and Grzegorz Cios for help with experimental investigations and numerous discussions, which made this work possible.

9. REFERENCES

[1] Isabell T C and Dravid V P 1997 *Ultramicroscopy* **67** 59-68
[2] Steinmetz D R and Zaefferer S 2010 *Mater. Sci. Technol.* **26** 640-645
[3] Zaefferer S 2007 *Ultramicroscopy* **107** 254-266
[4] Vespucci S, Winkelmann A, Naresh-Kumar G, Mingard K P, Maneuski D, Edwards P R, Day A P, O'Shea V and Trager-Cowan C 2015 *Phys. Rev. B* **92** 205301
[5] Keller R R and Geiss R H 2012 *J. Microscocopy* **245** 245-251
[6] Trimby P W 2012 *Ultramicroscopy* **120** 16-24
[7] Keller B 2013 What'sina'NYM? *Microscopy Today*, **21**(4) 72
[8] Sneddon G C and Trimby P W 2016 *Mater. Sci. Eng.* **110** 1-12
[9] Nolze G, Tokarski T, Cios G and Winkelmann A 2020 *J. Appl. Crystallogr.* **53** 435-443
[10] Rice K, Keller R R and Stoykovich M P 2015 *Microscopy Today* **23** 32-37
[11] Rice K, Keller R R and Stoykovich M P 2014 *J. Microscopy* **254** 129-136
[12] Tokarski T, Nolze G, Winkelmann A, Rychłowski Ł, Bała P and Cios G 2021 *Ultramicroscopy* **230** 113372
[13] Yuan H, Brodu E, Chen C, Bouzy E, Fundenberger J J and Toth L S 2017 *J. Microscopy* **267** 70-80
[14] Mortazavi N, Esmaily M and Halvarsson M 2015 *Mater. Lett.* **147** 42-45
[15] Trimby P W, Cao Y, Chen Z, Han S, Hemker K J, Lian J, Liao X, Rottmann P, Samudrala S, Sun J, Wang J T, Wheeler J and Cairney J M 2014 *Acta Materialia* **62** 69-80
[16] Tokarski T, Cios G, Kula A and Bała P 2016 *Mater. Char.* **121** 231-236
[17] Alonso G, Tokarski T, Stefanescu D M, Górny M, Cios G and Suarez R 2022 *Carbon* **199** 170-180